Indian Journal of Biochemistry & Biophysics
Vol. 62, October2025, pp. 1101-1110
DOI: 10.56042/ijbb.v62i10.16807

Quantitative estimation of Pyrophosphate ions released during loop-mediated isothermal amplification

Pulkit Srivastava, and Dinesh Prasad*
Department of Bioengineering and Biotechnology, Birla Institute of Technology, Mesra, Ranchi-835 215, Jharkhand, India

Received 31 January 2025; *revised 09 April 2025*

The increasing demand for rapid, sensitive, and instrument-free nucleic acid detection in clinical and field diagnostics necessitates innovative approaches for monitoring DNA amplification. Pyrophosphate ions (PPi) represent crucial targets generated during DNA and RNA polymerization, serving a pivotal role in monitoring real-time amplification processes and indirectly detecting various microorganisms. The Loop-Mediated Isothermal Amplification (LAMP) technique, known for its high sensitivity and user-friendly attributes, operates under isothermal conditions, eliminating the risk of PPi hydrolysis encountered in PCR. In this study, carbon dots were employed for the detection of PPi ions through an oxidation reaction involving o-Phenylenediamine (OPD) and hydrogen peroxide (H_2O_2). Blue-fluorescent carbon dots were synthesized using a hydrothermal method. Synthesized CDs acquired partial graphitic crystallinity with d-spacing values of 0.33 and 0.50 nm. Carbon and nitrogen were found in abundance in the CD structure. OPD (o-Phenylenediamine) and H_2O_2 react to form 2,3-Diaminophenazine (2,3-DAP) which is dark yellow while PPi blocks the electron transfer between these reactants and color change does not occur. Under UV light, it was found that fluorescence was quenched when PPi was not present between this reaction. While, in the presence of PPi, fluorescence was not quenched depicting that PPi blocks the formation of 2,3-DAP. The limit of Detection (LOD) and Limit of Quantitation (LOQ) for this technique was found to be around 50 nM and 190 nM. A standard plot, constructed using diverse concentrations of inorganic PPi, facilitated the quantification of PPi generated during LAMP at various time intervals and DNA concentrations.

Keywords: 2,3-diaminophenazine, Carbon dots, Diagnosis, DNA amplification, Limit of detection, O-phenylenediamine, *Salmonella*

Pyrophosphate (PPi) plays a vital role in various chemical and biological processes. It is formed during the hydrolysis of ATP under cellular conditions, DNA and RNA polymerization reactions, and many other biological processes[1,2]. During DNA and RNA polymerization, phosphodiester bonds are formed, resulting in the release of PPi. This serves as a key target for the detection of end-point and real-time amplification processes. Nucleic acids are important biomarkers for medical diagnostics and biological studies[3]. Loop-Mediated Isothermal Amplification (LAMP) is the most preferred technique in the field of biomolecular diagnostics after PCR[4]. Due to its rapid and high-yield results, it has secured a significant place in diagnostics. One of the main advantages of LAMP is that it can be used at any point-of-care (POC) site without the need for large equipment, facilitating the development of biosensors and detection kits[5].

PPi has been detected using various mechanisms such as colorimetric[6], turbidimetric[7], bioluminescent[8], and fluorometric methods[9]. When coupled with LAMP, these methods provide fast and accurate results. A study by Mori *et al*. (2004)[10] utilized turbidimetry, where DNA yields above 4 µg result in PPi reacting with magnesium in the reaction mix to form a white precipitate of $Mg_2P_2O_7$. Although PPi can hydrolyze at high temperatures, this is unlikely during LAMP due to its isothermal conditions.

In our study, we have adapted the method proposed by Chen *et al*. (2020)[2] to detect pyrophosphate. The method has been slightly modified and applied for the detection of DNA produced during LAMP using blue fluorescent carbon dots (CDs). Specific primers targeting the conserved region of *S. typhimurium* selectively amplify the target DNA, leading to the release of PPi. The redox reaction between O-phenylenediamine (OPD) and hydrogen peroxide (H_2O_2), catalyzed by the CDs, serves as an indicator for the reaction through a fluorescence quenching mechanism (Fig. 1).

The demand for rapid, sensitive, and specific nucleic acid detection has led to the development of

*Correspondence:
E-mail: dinesh@bitmesra.ac.in

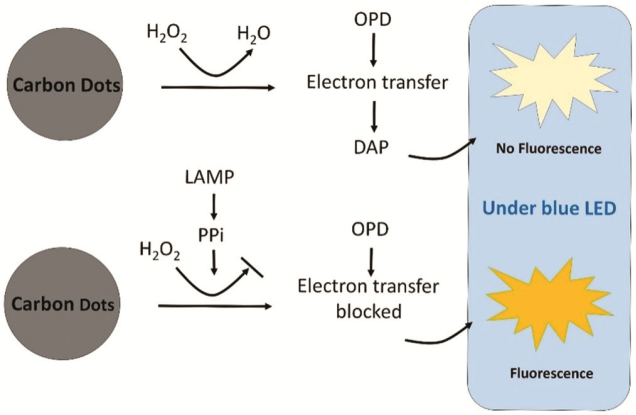

Fig. 1 — Schematic diagram representing the working of the developed technique. Reaction between O-phenylenediamine (OPD) and Hydrogen Peroxide (H_2O_2) leads to formation of 2,3-Diaminophenazine. Fluorescence of Carbon dots (CDs) quenches in absence of PPi during this reaction whereas CDs retains its fluorescence when PPi is present as electron transfer between OPD and H_2O_2 is blocked

isothermal amplification techniques, which offer advantages over conventional PCR, particularly in point-of-care and field-deployable diagnostic applications. Among these, LAMP has gained significant attention due to its high amplification efficiency, robustness, and ability to function under constant temperature without thermal cycling. A distinguishing biochemical feature of LAMP is the release of PPi as a by product of DNA synthesis, where the PPi quantity directly correlates with the amount of DNA amplified. Conventional LAMP detection methods such as turbidity, intercalating dyes, or real-time fluorescence often have limitations such as low quantifiability, non-specific signal generation, or the need for specialized instrumentation.

To address these challenges, recent advancements have focused on nanomaterial-based fluorescence sensing for PPi detection. Fluorescent nanomaterials[11] such as carbon dots[12], quantum dots[13], and dye-doped nanoparticles[14] offer high sensitivity, tunable optical properties, and fast responses. Carbon dots, in particular, are valued for their water solubility, photostability, biocompatibility, and ease of surface modification. Their fluorescence can be quenched by metal ions like Cu^{2+} and restored in the presence of PPi, forming stable complexes. This metal ion-mediated fluorescence modulation enables label-free, sensitive, and selective PPi detection at nanomolar levels.

Building upon these principles, we have developed method that couples LAMP amplification with carbon dot fluorescence sensing for real-time, visual, and quantitative detection of PPi. This platform eliminates the need for labelled probes or complex instruments and is ideal for use in resource-limited settings. In this study, we describe the design, optimization, and performance evaluation of the biosensor, highlighting its applicability for field-level diagnostics in clinical, agricultural, and environmental contexts.

Materials and Methodology

Materials

Phosphate assay kit, O-phenylenediamine (99%) (OPD), and Sodium Pyrophosphate Decahydrate were purchased from Sigma-Aldrich. Lyophilized culture of *S. typhimurium* (MTCC 98) was procured from IMTECH, Chandigarh, India. Specific LAMP primers for *S. typhimurium* were purchased from Eurofins Genomics, India. *Bst* DNA Polymerase and Thermopol Buffer were purchased from New England Biolabs. Quinine sulfate was purchased from HiMedia.

Synthesis and Characterization of CDs

CDs were prepared by the hydrothermal method described by Chen *et al* 2020[2] through the Maillard reaction of precursors which finally resulted in nano-sized particles. Briefly, 10 mM D-Galactose and 120 mM L-histidine were mixed with 0.1 M NaOH in 20 mL water in an Erlenmeyer flask and then kept on a hot plate at 100°C for 12 h with 1000 rpm stirring. After 12 h, the brown solution was cooled to room temperature, centrifuged at 12000 rpm for 20 min to remove large particles, and filtered through 0.22 µM syringe-driven filters. The obtained solution was checked under 395 nm UV light and then kept at 4°C. UV-vis absorbance spectra from 200-700 nm were performed on LAB INDIA, 3100-XE spectrophotometer, Department of Bioengineering and Biotechnology, BIT Mesra, Ranchi, India. Band Gap for the CDs was obtained using absorbance spectra of CDs using Origin 8.5.

KBr pellets were prepared using a pelletizer with CDs powder and Fourier Transform Infrared Spectra (FTIR) from 4000 to 500 cm^{-1} was obtained from IR-Prestige 21, Shimadzu Corp. (Tokyo, Japan). Size Distribution and Zeta Potential of CDs were obtained from Nano Zetasizer, Malvern Instruments. XRD pattern of CDs was obtained from SmartLab 9kW, Rigaku, Japan. Fluorescence Spectra was performed on an excitation wavelength of 320 nm on RF-5301, Shimadzu, Japan. EDAX spectra were obtained from Sigma 300, Ametek. All these results were obtained from the Central Instrumentation Facility, Department

of Bioengineering and Biotechnology, BIT, Mesra, Ranchi, Jharkhand, India. HR-TEM images were obtained using the FEI Tecnai TF20 electron microscope from the Central Research Facility, Indian Institute of Technology, Delhi, India. HR-TEM image analysis was done in ImageJ software. The Quantum Yield of synthesized CDs was detected using Quinine sulfate as a reference[15]. Quinine sulfate (QS) being a fluorophore resembles the fluorescence of CDs. For QY, five concentrations of QS were dissolved in 0.1 N H_2SO_4 which has absorbance less than 0.1 nm. CDs were dissolved in water and absorbance was taken. QY was calculated using the following equation[16].

$$\emptyset ST = \emptyset x \left(\frac{mx}{mSt}\right)\left(\frac{\eta 2x}{\eta 2ST}\right) \text{(Eq. 1)}$$

Primer Designing andLAMP

Primer Explorer V5 was used to design primers targetingthe*stn*gene which is specific to all *Salmonella sp.* listed in (Table 1). To prepare LAMP reaction mix, Thermopol buffer (1X), dNTP's (0.4 M each), *Bst* DNA polymerase (1 U), FIP and BIP (1.6 µM), F3 and B3 (0.4 µM), LF and LB (0.8 µM) and 0.8 M betaine were mixed with template DNA (1 µL) of *S. typhimurium* and reaction was performed at 60°C for 60 min. DNA bands were observed in 1.5% agarose gel under the Gel-Doc system.

Detection of PPiand Sensitivity

25 mM OPD, prepared in 95 % acetate buffer (0.1 M, pH 4.0), and 5% DMSO and 250 mM H_2O_2 were used for the oxidation reaction. Briefly, 150 µL of OPD and 30 µL of H_2O_2 were mixed and kept at ambient temperature (35°C) for 10 min. The same reaction was done in the presence of 30 µL of CDs (0.5 µg/mL in acetate buffer). 30 µL of 1000 µM inorganic pyrophosphate (Prepared using sodium pyrophosphate decahydrate in acetate buffer pH 4.0, 0.1M) solution was used to block the electron transfer between OPD and H_2O_2 in the presence and absence of CDs. After 10 min, Fluorescence spectra were taken for OPD+CDs+PPi+H_2O_2 and OPD+CDs+H_2O_2 at the excitation wavelength of λ_{ex}=350 nm.

Different concentrations of Inorganic pyrophosphate solution were prepared (0.05 µM to 1000 µM) by mixing in acetate buffer (0.1 M, pH 4.0). Absorbance spectra of different concentrations of inorganic PPi were taken in the range of 600-350 nm along with OPD, H_2O_2, and CDs. Visible detection of fluorescence quenching was seen under 395 nm UV light. A Linear graph was plotted using absorbance vs concentration data. LOD and LOQ were calculated using the 3σ/m and 10σ/m method where σ is the standard deviation and m is the slope[17].

Confirming the presence of PPi in LAMP

DNA was amplified using LAMP to check the presence of PPi in LAMP using a phosphate assay kit. LAMP was performed at 10, 20, 30, 40, 50, and 60 min and a control was kept as a non-amplified LAMP reaction mix with DNA.

Quantitation of PPi

PPi released during LAMP was quantified using a standard curve prepared using different concentrations of sodium pyrophosphate decahydrate dissolved in acetate buffer (0.1 M and pH 4.0). LAMP was performed at different time intervals (10, 20, 30, 40, 50, and 60 min) to check the quantity of PPi released at each point. A calibration curve prepared using the PPi standard is used to calculate PPi concentration in the amplified and non-amplified reaction mix. Amplified LAMP mixture was visualized using gel electrophoresis and carbon dots. PPi concentration was also calculated at different DNA concentrations. First, absorbance for DNA was taken at 260 nm and concentration was calculated using the below formula:

DNA Concentration (µg/mL) = OD_{260}×Conversion factor (Eq. 2)

Here the conversion factor for double-stranded DNA is 50. DNA was diluted 10 times up to 10^{-4}

Table 1 — Primers and their sequence used for amplification of *S. typhimurium* through LAMP

S. No	Primers	Sequence (5′ to 3′)	bp Length	Position
1	FIP	ATTCATGCGATTGGCCGCCAG-TGATGATAACGCGGTCGGT	40	616-636, 564-582
2	BIP	TCAACAGCACCTGAGTCAGCC-AGATTCACGGCGAATGAGAC	41	654-674, 704-723
3	F3	CCTTTCCCGCTATCGGTAAC	20	542-561
4	B3	GGATGCCCAAAGCAGAGAG	19	733-751
5	LF	CGTAGAGGCAAAAGAAAGTGGG	22	583-604
6	LB	TGTCCGGGTCAGCCTGAATAC	21	675-695

concentration and LAMP was performed for 60 min at 60°C.

Results

Synthesis and characterization of carbon dots

Carbon dots synthesized using the hydrothermal method show blue fluorescence under 395 nm UV light (Fig. 2A).The solution was lyophilized to obtain the powder form of CDs for further characterization. UV-vis spectrum shows absorbance in the UV region within the range of 230 to 350 nm (λ_{max}=230 nm) with a tail extending into the visible region (Fig. 2B), whereas the highest peak was present at 230 nm attributed to π- π* transition of C=C band and a shoulder peak at 333 nm is attributed to η- π* of C=O band[18,19]. Fluorescence spectra show λ_{em} at 440 nm when excited with a wavelength of λ_{ex}=350 nm (Fig. 2C). The band Gap for the synthesized CDs was found to be around 3.86 eV (Fig. 2B inset).

The hydrodynamic size distribution of CDs shows a Z-average of 144 nm ranging from 18.17 nm to 531.2 nm (Fig. 3A) representing different sized and aggregated particles whereas zeta potential was found to be around -17.5 mV confirming the presence of negative surface charge and long-term stability (Fig. 3B). FTIR spectra show a peak at 3182.5 attributed to stretching vibrations of the OH alcohol group while a peak at 2777.9 is attributed to H-C=O:C-H stretching aldehydes. The peak at 1693.5 shows the presence of NH bend amines and 1400.32 is attributed to C-C stretching aromatics. 1392.5 shows the presence of CN stretching aliphatic amines (Fig. 3C). FTIR spectra show the presence of mostly COO^- and NH^{3+} functional groups suggesting the composition of CDs is mostly made up of carbon and nitrogen. This data is supported by Elemental analysis and EDAX which shows the presence of Carbon and Nitrogen in abundant amounts. The elemental analysis report shows a C/N ratio of 4.238 with C% (45.72), N% (10.79), and H% (6.325). EDAX analysis report shows the presence of C and N in weight % of 59.86 and 40.14 (Fig. 3D). XRD spectra show a broad 2θ peak at 17.58° with a shoulder peak at 27.34° while the d-spacing of both values was found to be 0.50 nm and 0.33 nm (Fig. 3E). The broad peak at 17.58° confirms the amorphous nature of CDs and the d-spacing value of 0.50 nm is much higher than the graphitic plane. The shoulder peak at 27.34° has a d-spacing value of 0.33 nm which is similar to the graphitic plane (100) suggesting that CDs can acquire partial graphitic crystallinity[1]. This was further confirmed by the HRTEM image and SAED pattern of CDs.

HRTEM image of synthesized CDs shows a crystalline nature with a d-spacing of 0.33 nm corresponding to the lattice fringes of (002) planes (Fig. 3F). Due to the high agglomeration property of CDs, it was difficult to discern the shape. HRTEM results of CDs suggested that a certain number of crystals were formed, although XRD spectra show the amorphous nature of CDs[20,21]. SAED pattern shows crystalline spots with amorphous rings suggesting that synthesized CDs acquired partial graphitic crystallinity[22,23](Fig. 3G).

Quantum yield calculated using fluorescence spectra of CDs and reference material quinine sulfate (54 %) was found to be around 24.64% which was higher than some of the previously reported carbon dots. These CDs demonstrated intrinsic peroxidase-like activity, catalyzing the oxidation of o-phenylene-diamine (OPD) in the presence of hydrogen peroxide (H_2O_2) to form 2,3-diaminophenazine (DAP), a yellow-colored product with a strong absorbance at 450 nm.

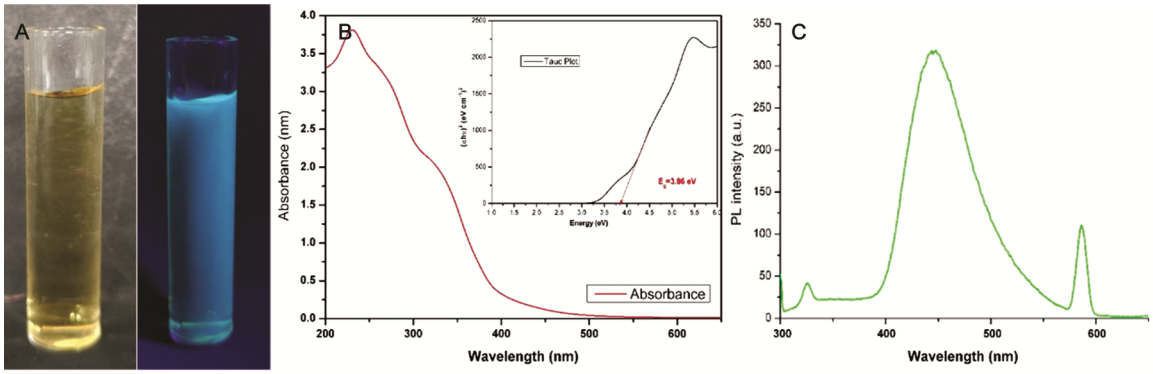

Fig. 2 — Synthesis and optical properties of carbon dots. (A) Synthesized carbon dots showing blue fluorescence under 395 nm UV light; (B) The absorbance of CDs with λ_{max}=230 nm and band gap (inset) of carbon dots with an energy gap of 3.86 eV; and (C) Fluorescence spectra of CDs showing λ_{em}= 440 nm at λ_{ex}= 350 nm

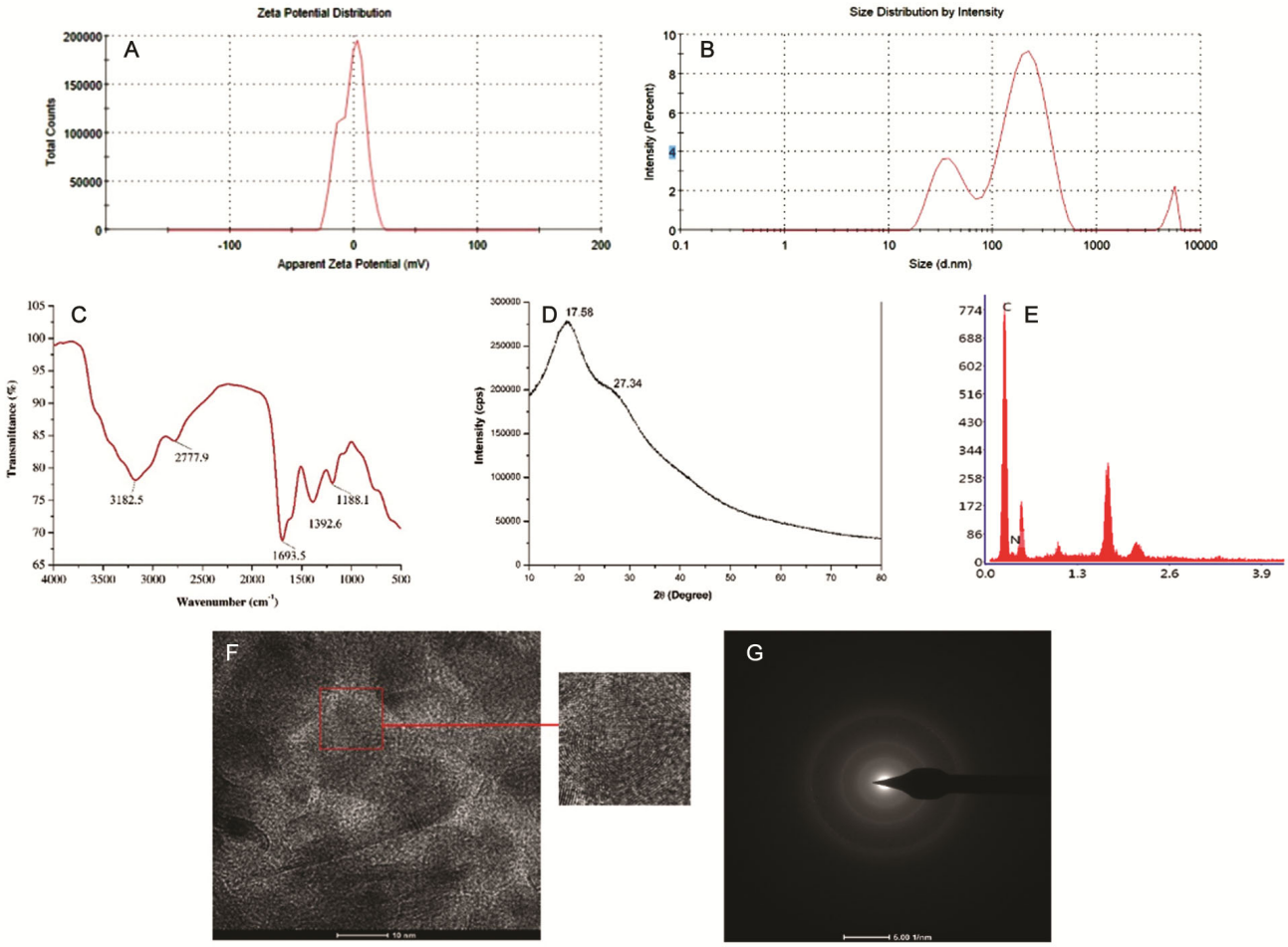

Fig. 3 — Morphological properties of synthesized carbon dots (A) Size distribution histogram showing z-average of 144 nm; (B) Zeta potential of CDs was found to be -17.5 mV, (C) FTIR spectra shows the presence of COO^- and NH_3^+ functional groups; (D) XRD spectra showing broad amorphous peak at 17.55 with a shoulder peak at 27.34; (E) EDAX spectra shows presence of Carbon and Nitrogen in abundant amount; (F) HRTEM showing crystal lattice spacing of 0.33 nm which is same to graphitic plane showing CDs also acquire graphitic crystallinity; and (G) SAED pattern showing partial graphitic crystallinity

The detection chemistry is based on PPi-induced inhibition of the CDs' catalytic activity. In the absence of PPi, CDs facilitate electron transfer from OPD to H_2O_2, generating a colorimetric signal via DAP formation. However, when PPi is present, it binds selectively to functional groups primarily amino and carboxylic acid moieties on the CD surface. This binding blocks the active sites involved in catalysis, disrupting electron transfer and thereby inhibiting DAP formation. The inhibition results in a loss of yellow color and serves as a direct indicator of PPi presence and concentration (Fig. 1). The detection of PPi has attracted significant attention due to its biological relevance as a by-product of DNA and RNA polymerization reactions, including LAMP. The integration of nanotechnology with molecular diagnostics has introduced innovative sensing strategies, among which CDs serve as a promising platform owing to their exceptional optical and surface properties. This approach provides a robust, label-free alternative to conventional fluorescence-based nucleic acid assays. Furthermore, its adaptability to portable formats enhances its potential for point-of-care diagnostics and environmental monitoring.

Detection of pyrophosphate and sensitivity

OPD solution is generally transparent but when it reacts with H_2O_2, it forms 2,3-diamino phenazine (DAP) turning the solution into a dark yellow color. But when PPi is introduced into the solution, it blocks the electron transfer between H_2O_2 and OPD inhibiting color change. (Figs 1 & 4A). In fluorescence spectra, higher emission was observed when PPi was present while a lower emission peak

was observed in the absence of PPi (Fig. 4B). CDs work as a catalytic agent of the reaction, and their fluorescence works as an indicator for detecting pyrophosphate ions in a solution.

LOD and LOQ calculation was performed using the absorbance of different concentrations of PPi (0.05 µM to 1000 µM). A lower concentration was taken to get a linear fit curve which is required for the calculation of LOD and LOQ.

Fluorescence for different concentrations of PPi can be seen under 395 nm UV light. Higher fluorescence was observed towards higher concentrations of PPi while fluorescence quenching can be seen towards lower concentrations of PPi (Fig. 5A). The linear regression graph shows a good linear relationship with an R^2 value of 0.997 and y=0.356x+0.222 (Fig. 5B & C). LOD and LOQ calculated using these values were found to be 50 nM and 190 nM. A recent study based on the detection of Pyrophosphate ions in LAMP shows an LOD of 1.73 µM[24] while our study shows an LOD of 50 nM.

Confirming the presence of PPi in LAMP

DNA was amplified using LAMP to check the presence of PPi in LAMP using a phosphate assay kit. The dark green color formation was seen increasing towards 60 min amplification time confirming the increase in concentration of PPi. No change in color was observed in control confirming that PPi is released during amplification of DNA (Fig. 6A). In agarose gel, dense DNA bands can be seen in 40, 50, and 60 min whereas no bands were observed in 10, 20, and 30 min amplification time (Fig. 6B). This signifies that the agarose gel electrophoresis was not able to detect amplified DNA in lower amplification time but dark green color formation in phosphate assay shows release of PPi.

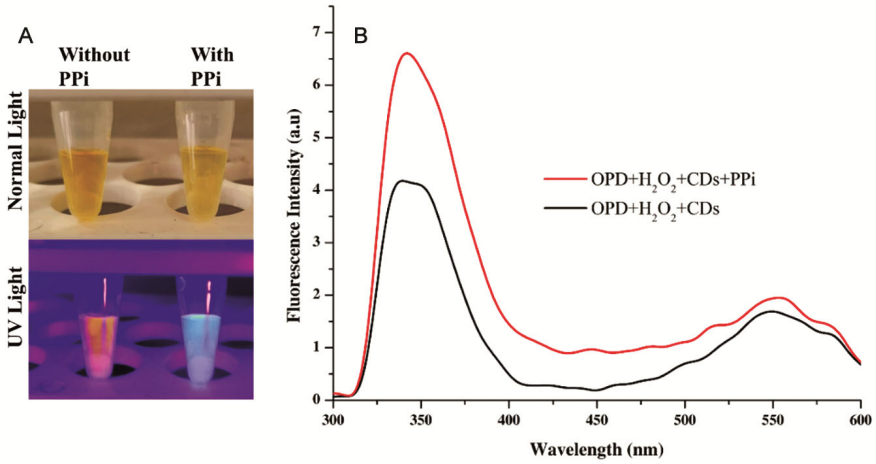

Fig. 4 — Detection of inorganic PPi (A) Oxidation reaction between OPD and H_2O_2 under normal light and UV light in presence of carbon dots. Blue fluorescence is quenched under absence of PPi while carbon dots retained its blue fluorescence in the presence of PPi; and (B) Fluorescence spectra showing decreased fluorescence emission in absence of PPi

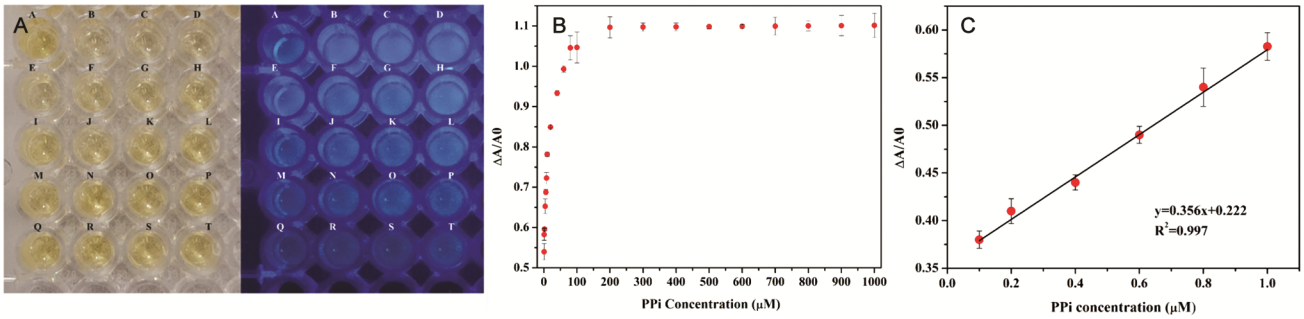

Fig. 5 — Sensitivity of the PPi detection technique (A) Different concentration of PPi with OPD+H_2O_2+CDs (A-Control, B- 0.05 µM, C-0.1 µM, D-0.2 µM, E-0.4 µM, F-0.6 µM, G-0.8 µM, H-1 µM, I-2.5 µM, J-5 µM, K-10 µM, L-25 µM, M-50 µM, N-75 µM, O-100 µM, P-200 µM, Q-400 µM, R-600 µM, S-800 µM, T-1000 µM); (B) Absorbance of Different concentration of PPi from 0 µM to 1000 µM at 440 nm; and (C) Linear fit graph of different concentration of PPi from 0.1 µM to 1µM. LOD and LOQ calculated using this linear fit graph was found to be 50 nM and 190 nM

Quantitation of PPi in different conditions

Firstly, we have confirmed the presence of PPi in LAMP using a phosphate assay kit at different time intervals. The formation of a dark green color confirms the presence of PPi after amplification. The difference in DNA bands is observed in agarose gel where no band was observed in control (non-amplified reaction mix), at 10 and 20 min while light to dark bands were observed at 30,40, 50, and 60 min. Fluorescence was observed in different time intervals while fluorescence was quenched in the control (Fig. 7). The concentration of PPi calculated is listed in (Table 2).

PPi concentrations were also quantified for different DNA concentrations up to 10^{-4}. The concentration calculated for DNA was found to be 52 µg/mL. The concentration of PPi found at each DNA concentration is listed in (Table 3). The fluorescence of carbon dots can be seen quenching towards lower DNA concentration signifying a low amount of PPi (Fig. 8).

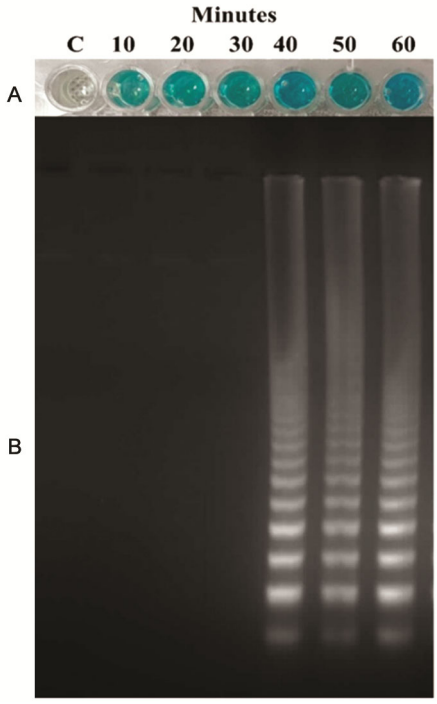

Fig. 6 — Visual confirmation of PPi presence in LAMP. (A) Phosphate assay showing formation of dark green color towards higher amplification time where C is control having non amplified reaction mix; and (B) Gel electrophoresis image after LAMP where no bands can be seen in C and at 10, 20 and 30 min anddense bands can be seen at 40, 50 and 60 min

Table 2 — Concentration of PPi released during LAMP at different time intervals

Time (Min)	Mean Abs. (440 nm)	PPi Concentration (µM)
10	0.52 ± 0.03	1.10 ± 0.85
20	0.61 ± 0.01	3.51 ± 0.32
30	0.73 ± 0.02	6.82 ± 0.77
40	0.81 ± 0.03	8.96 ± 1.0
50	0.95 ± 0.02	12.53 ± 0.61
60	1.3 ± 0.08	21.91 ± 2.3

Table 3 — Concentration of PPi released during LAMP at different DNA Concentrations.

DNA Concentration (ng/mL)	Mean Abs. (440 nm)	PPi Concentration (µM)
52000	1.19 ± 0.031	22.45 ± 0.85
5200	1.05 ± 0.038	18.79 ± 1.02
520	0.85 ± 0.032	13.43 ± 0.87
52	0.67 ± 0.032	8.52 ± 0.87
5.2	0.52 ± 0.029	4.52 ± 0.78

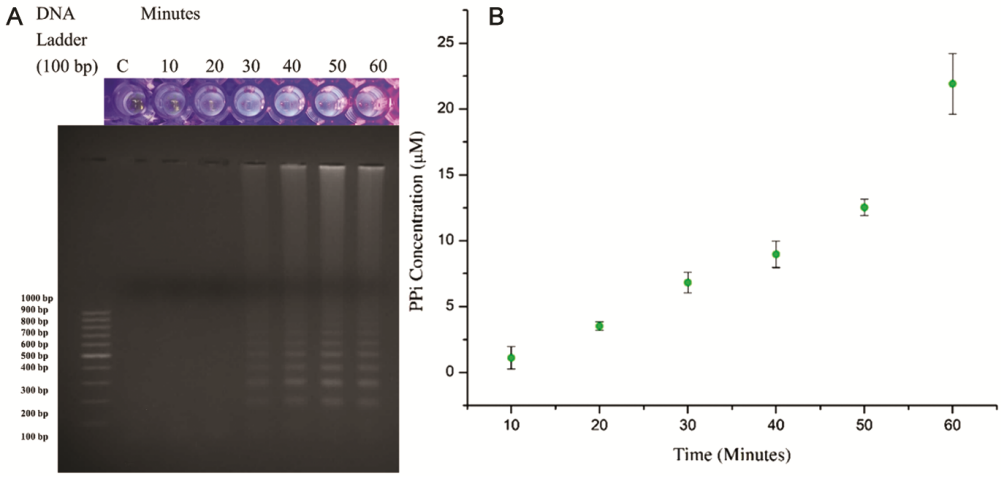

Fig. 7 — Quantification of PPi produced in LAMP at different time intervals (A) 1.5% agarose gel image showing no bands at 10 and20min while light to dark bands can be seen at 30,40, 50 and 60 min where C is control with non-amplified reaction mix to compare production of PPi. Higher fluorescence can be seen towards higher amplification time where C is control; and (B) Amplification time *vs* PPi Concentration (µM) graph at 440 nm showing increasing concentration of PPi with increase in amplification time

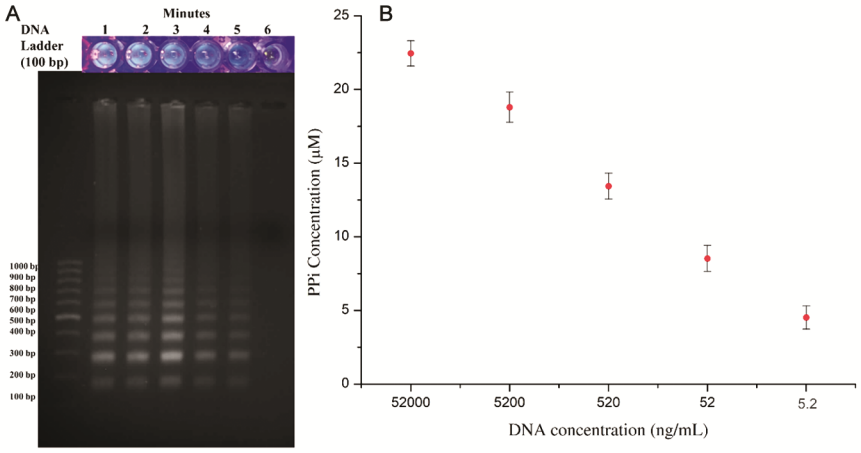

Fig. 8 — Effect on PPi concentration in different DNA dilution method (A) 1.5% agarose gel image showing darker to lighter bands towards lower DNA concentration. (DNA Conc. in ng/mL: 1-52000; 2-5200; 3-520; 4-52; 5-5.2; 6-Control). Fluorescence can be seen quenching towards lower DNA concentration; and (B) DNA concentration *vs* PPi concentration graph 440 nm showing decrease in PPi concentration towards lower DNA concentration

As the concentration of PPi released during LAMP is very high, it is easier to detect PPi using carbon dots because of its high sensitivity. LAMP produces a high no. of copies of DNA in low time intervals which may not be detected using Agarose gel electrophoresis but carbon dots assay can provide visible positive results in less time. It can also be seen that LAMP produces a higher amount of PPi ions than PCR due to isothermal conditions which allow PPi not to get hydrolysed in amplification conditions.

Discussion

Traditional methods for detecting inorganic PPi in biological samples and during/after DNA amplification primarily include colorimetric, fluorometric, electrochemical, and electrophoretic techniques. Colorimetric methods, such as the molybdate assay, rely on the formation of a blue complex between PPi and molybdate under acidic conditions. Based on this protocol developed by Tomita *et al*. 2008[25], Chen *et al*. (2022)[26] developed a portable and stable on-site device for rapid detection of *Enterocytozoon hepatopenaei* using LAMP. The optimal absorbance range for detecting LAMP products was 555–655 nm. This method incorporates a laser diode enhanced signal stability and accuracy with a detection limit as low as 0.1 fg/µL. These are simple and cost-effective but often lack sensitivity and can suffer from phosphate interference. Yang *et al*. (2025)[6] developed a colorimetric method for PPi detection based on an anti-etching mechanism involving gold nanorods (Au NRs) and Fe^{3+} ions. In acidic conditions, Fe^{3+} etches Au NRs, causing a visible color shift from blue to pink. However, in the presence of PPi, Fe^{3+} preferentially binds to PPi, preventing Au NR etching and preserving their morphology. The method, aided by SCN^- complexation, offers high selectivity, a naked-eye LOD of 3 µM, and a UV–vis-based LOD of 1.93 µM, with results obtainable within 15 min.

Fluorometric assays offer greater sensitivity, commonly using enzymes like ATP sulfurylase to convert PPi into ATP, which can then be detected using luciferase-based fluorescence. The ATP sulfurylase assay demonstrated an analytical sensitivity range of 0.15 to 10 µM for inorganic pyrophosphate (PPi), with both inter- and intra-assay coefficients of variability remaining below 10%, indicating high reproducibility and reliability. Using this method, Bernhard *et al*. (2022)[27] established a reference range for plasma PPi levels in children and adolescents aged 0 to 18 years. The standard range was determined to be between 2.36 and 4.44 µM, with a median value of 3.17 µM. The study by Yang *et al*. (2021)[28] demonstrated the remarkable sensitivity and broad detection range of BPHA carbon dots (CDs) for pyrophosphate (PPi) detection via a fluorescence turn-on mechanism. Upon increasing Cu^{2+} concentrations up to 2100 µM, 97% of the initial fluorescence of BPHA CDs was quenched. This method could detect 4400 µM of PPi in complex biological samples such as urine. Shi *et al*. (2021)[29] reported a fluorescence-based PPi detection method using Cu^{2+} modified gold nanoclusters (AuNCs) with a linear range of 1–300 µM and a limit of detection (LOD) of 0.82 µM. Bhowmik *et al*. (2014)[30] reported a simple terpyridine-Zn(II) complex as a highly selective and

sensitive fluorescent sensor for pyrophosphate (PPi) in water at physiological pH. The sensor exhibited an exceptional fluorescence enhancement (~500-fold) with a low detection limit of ~0.8 nM.

Slater *et al*. (2023)[31] developed a rapid and sensitive LAMP-based electrochemical assay for SARS-CoV-2 detection by leveraging the redox reaction between LAMP-generated pyrophosphate and molybdate, measured via cyclic voltammetry on low-cost carbon screen-printed electrodes. The assay demonstrated a limit of detection as low as 100 attograms of RNA (equivalent to 5.29 RNA copies/μL), which is significantly more sensitive than conventional fluorescence-based RT-LAMP. Validated using spiked human serum, saliva, and clinical swab samples. However, the LAMP-based electrochemical assay offers high sensitivity, its reliance on electrochemical sensors and cyclic voltammetry necessitates specialized equipment and trained personnel, limiting its suitability for POC or field settings compared to simpler, label-free visual detection methods. A study presents a metal-free, highly sensitive, and selective method for pyrophosphate (PPi) detection using nanozymatic carbon dots. The CDs mimic peroxidase activity, which is selectively inhibited by PPi, enabling both colorimetric and portable paper-based detection with a low detection limit of 4.29 nM^2. In contrast, our approach matches or exceeds many of these in terms of detection limit (50nM-190-nM), while maintaining ease of use, faster turnaround time, and compatibility with low-resource settings. Furthermore, unlike electrochemical techniques requiring specialized equipment, or hydrogel-based paper strips requiring imaging, our platform can be adapted for direct visual or fluorescence-based readout, making it equally effective and more accessible for routine or point-of-care PPi monitoring.

The developed PPi detection platform demonstrates higher sensitivity. However, its application to complex clinical or environmental samples presents certain challenges that needs consideration. In such complex matrices, the presence of amplification inhibitor such as humic acids, heme, or polysaccharides can interfere with the efficiency of the LAMP reaction, subsequently reducing the amount of PPi generated. Moreover, low target DNA concentrations and variability in extraction efficiency may further compromise the reliability of amplification and further downstream results.

Once successful LAMP amplification occurs, the release of PPi serves as an indirect but reliable proxy for the presence of target DNA. However, the detection of PPi *via* fluorescence quenching of blue carbon dots still faces challenges in post amplification reactions. That includes salts, buffer, and other biological components (such as proteins, DNA, RNA) may interfere with the fluorescence of carbon dots, while quenching agents or background fluorescence can hide signal interpretation. To address these issues, we may optimize DNA extraction protocols, incorporating inhibitor removal steps, and exploring signal normalization strategies using internal references.

Conclusion

Carbon dots synthesized using precursors Galactose and Histidine show blue fluorescence. Synthesized carbon dots acquired partial graphitic crystallinity which is one of the unique properties of some carbon dots. PPi produced during LAMP forms a white precipitate when in higher concentrations. However, the precipitate needs to be settled down before visual detection for which centrifugation-type steps are needed. This assay provides much better sensitivity and ease of detection even in low concentrations of PPi. This method can be useful in detecting various pathogens only if aspecific primer is provided. Also, this can be implemented with paper-based microfluidics to reduce the cost of detection and easy handling by non-skilled personnel at POC sites.

Acknowledgement

PSis grateful to the Department of Bioengineering and Biotechnology, Birla Institute of Technology, Mesra, Ranchi for providing the Institute Research Fellowship (GO/IRF/2019-20/4349). DP is thankful to Birla Institute of Technology, Mesra, Ranchi for the seed money grant (GO/Estb/SMS/2019-20/2122) provided for this research.

Conflict of interest

Both the authors declare no conflict of interest.

References

1 Liu Y, Zhou Q, Yuan Y & Wu Y, Hydrothermal synthesis of fluorescent carbon dots from sodium citrate and polyacrylamide and their highly selective detection of lead and pyrophosphate. *Carbon*, 115 (2017) 550.

2 Chen CY, Tan YZ, Hsieh PH, Wang CM, Shibata H, Maeijima K, Wang TY, Hiruta Y, Citterio D & Liao WS, Metal free colorimetric detection of pyrophosphate ions by inhibitive nanozymatic carbon dots, *ACS Sens*, 5 (2020) 1314.

3 Yan L, Zhou J, Zheng Y, Gamson AS, Roembke BT, Nakayama S &Sintim HO, Isothermal amplified detection of DNA and RNA. *Mol Bio Syst*, 10 (2014) 970.

4 Notomi T, Okayama H, Masubuchi H, Yonekawa T, Katanabe K, Amino N & Hase T, Loop-mediated isothermal amplification of DNA. *Nucleic Acids Res*, 28 (2000) E63.

5 Yang N, Zhang H, Han X, Liu Z & Lu Y, Advancements and applications of loop-mediated isothermal amplification technology: a comprehensive overview. *Front Microbiol*, 15 (2024) 1406632.

6 Yang Y, Peng M, Zang W, Jiang Y, Miao L, Wang C, Zhang Y, Wu A & Zhang Y, Colorimetric detection of pyrophosphate using gold nanorods and Fe^{3+} based on anti-etching mechanism, *Colloids Surf A Physicochem Eng Asp*, 704 (2025) 135486.

7 Hokazono E, Fukumoto S, Uchiumi T & Osawa S, Pyrophosphate detection method using 5-Br-PAPS to detect nucleic acid amplification - Application to LAMP method. *Anal Biochem*, 684 (2024) 115371.

8 Tan G, Fei Z, Wei R, Wu X & Xiao P, Development of a Novel Bioluminescence Pyrophosphate Assay for the High-Sensitivity Detection of Hepatitis B Virus, *Appl Biochem Biotechnol*, 194 (2022) 725.

9 Xu Q, Xiao F & Xu H, Fluorescent detection of emerging virus based on nanoparticles: From synthesis to application. *TrAC Trends in Anal Chem*, 161 (2023) 116999.

10 Mori Y, Kitao M, Tomita N &Notomi T, Real-time turbidimetry of LAMP reaction for quantifying template DNA. *J Biochem Biophys Meth*, 59 (2004) 145.

11 Wang Y, Xia K, Wang LC, Wu MX, Sang XJ, Wan KM, Zhang XD, Liu XM & Wei G, Peptide-Engineered Fluorescent Nanomaterials: Structure Design, Function Tailoring, and Biomedical Applications. *Small*, 17 (2021) 2005578.

12 Garg R & Prasad D, Enhanced pyrophosphate detection: Utilizing oPD-derived carbon dots and Fe^{3+} interactions in a paper strip biosensor. *Biochem Biophys Res Commun*, 739 (2024) 150577.

13 Zhang Y, Liu Y, Yang Y, Li L, Tao X & Song E, Rapid detection of pathogenic bacteria based on a universal dual-recognition FRET sensing system constructed with aptamer-quantum dots and lectin-gold nanoparticles. *Chi Chem Lett*, 34 (2023) 108102.

14 Mondal S & Dey N, Exploring photophysical properties of organic doped polymeric aggregates for detecting relevant inorganic pyrophosphate: A pathway to sustainable development. *J Env Chem Eng*, 12 (2024) 114412.

15 Alkian I & Sutanto H, Quantum yield optimization of carbon dots using response surface methodology and its application as control of Fe^{3+} ion levels in drinking water. *Mater Res Express*, 9 (2022) 015702.

16 Algi F, Algi MP, Sonkaya Ö & Ocakçı S, Luminescent carbon dots endowed with selective recognition of the carcinoid tumor biomarkers in biological fluids. *Dyes Pigm*, 230 (2024) 112333.

17 Uhrovcik J, Strategy for determination of LOD and LOQ values-Some basic aspects. *Talanta*, 119 (2014) 178.

18 Gao Y, Jiao Y, Lu W, Liu Y, Han H, Gong X, Xian M, Shuang S &Dong C, Carbon dots with red emission as a fluorescent and colorimetric dual-readout probe for the detection of chromium (vi) and cysteine and its logic gate operation. *J Mater Chem*, 6 (2018) 6099.

19 Wang Y, Chang X, Jing N & Zhang Y, Hydrothermal synthesis of carbon quantum dots as fluorescent probes for the sensitive and rapid detection of picric acid. *Anal Meth*, 10 (2018) 2775.

20 Liang Z, Kang M, Payne GF, Wang X & Sun R, Probing Energy and Electron Transfer Mechanisms in Fluorescence Quenching of Biomass Carbon Quantum Dots. *ACS Appl Mater Inter*, 8 (2016) 17478.

21 Asadzadeh-Khaneghah S, Habibi-Yangjeh A & Nakata K, Decoration of carbon dots over hydrogen peroxide treated graphitic carbon nitride: exceptional photocatalytic performance in removal of different contaminants under visible light. *J Photochem and Photobio A: Chem*, 374 (2019) 161.

22 Pal A, Sk MP & Chattopadhyay A, Recent advances in crystalline carbon dots for superior application potential. *Mater Adv*, 1 (2020) 525.

23 Mandal S & Das P, Are carbon dots worth the tremendous attention it is getting: Challenges and opportunities. *Appl Mater Today*, 26 (2022) 101331.

24 Arumugam SS, Nair SS, Varghese AW, Usha A, Varghese RE, Joseph R & Thekkuveettil A, Dual-Emissive Carbon Dots: Exploring Their Fluorescence Properties for Sensitive Turn-Off–On Recognition of Ferric and Pyrophosphate Ions and Its Application in Fluorometric Detection of the Loop-Mediated Isothermal Amplification Reaction. *Langmuir*, 39 (2023) 5779.

25 Tomita N, Mori Y, Kanda H & Notomi T, Loop-mediated isothermal amplification (LAMP) of gene sequences and simple visual detection of products. *Nat Protoc*, 3 (2008) 877.

26 Chen Z, Zhao K, He Z, Luo X, Qin Z, Tan Y, Zheng X, Wu Z, Deng Y, Chen H, Guo Y & Li S, Development and evaluation of a thermostatic nucleic acid testing device based on magnesium pyrophosphate precipitation for detecting *Enterocytozoon hepatopenaei*. *Chi Chem Lett*, 33 (2022) 4053.

27 Bernhard E, Nitschke Y, Khursigara G, Sabbagh Y, Wang Y & Rutsch F, A reference range for plasma levels of inorganic pyrophosphate in children using the ATP sulfurylase method. *J Clin Endocrin Metabol*, 107 (2022) 109.

28 Yang Y, Chen P, Liu Y, Cai Z, Wang X, Me Y, Ding X, Lin L, Jiang H, Zhang Z & Ju Y, A colorimetric indicator-displacement assay based on stable Cu^{2+} selective carbon dots for fluorescence turn-on detection of pyrophosphate anions in urine. *Spectrochim Acta A Mol Biomol Spectrosc*, 251 (2021) 119479.

29 Shi Y, Wang J, Mu K, Liu S, Yang G, Zhang M & Yang J, Copper (II) ion-modified gold nanoclusters as peroxidase mimetics for the colorimetric detection of pyrophosphate. *Sensors*, 21 (2021) 5538.

30 Bhowmik S, Ghosh BN, Marjomaki V & Rissanen K, Nanomolar pyrophosphate detection in water and in a self-assembled hydrogel of a simple terpyridine-Zn2+ complex. *J Am Chem Soc*, 136 (2014) 5543.

31 Slater KB, Ahmad M, Poirier A, Stott A, Siedler BS, Brownsword M, Mehat J,Urbaniec J, Locker N, Zhao Y, Ragione RL, Silva SRP & McFadden J, Development of a loop-mediated isothermal amplification (LAMP)-based electrochemical test for rapid detection of SARS-CoV-2. *iScience*, 26 (2023) 107570.